Ioffe Institute
6th Int. Symp. "Nanostructures: Physics and Technology"
St Petersburg, Russia, June 22–26, 1998.

InGaAs quantum wires in [110] and [1$\bar{1}$0] gratings: two V-grooves directions, two behavior of the regrowth interface

C. Gourgon†, F. Filipowitz†, J. Robadey†, D. Martin†, Y. Magnenat†, P. C. Silva†, F. Bobard‡ and F. K. Reinhart†

† Institute of Micro- and Optoelectronics
‡ Center of Electron Microscopy
Federal Institute of Technology, CH-1015 Lausanne, Switzerland

Abstract. InGaAs quantum wires are obtained by holographic lithography and MBE regrowth on V-grooves. The influence of some fabrication steps on the interface is presented. The [110] and [1$\bar{1}$0] gratings are compared in terms of etching profiles and the evolution of the grating shape during the desorption and the epitaxial regrowth.

1 Introduction

There is great interest in reducing the physical size of semiconductor structures to take advantage of quantum effects for optical and optoelectronic applications. Semiconductor wires are expected to result in sharp gain and absorption spectra. Quantum wires grown on patterned substrates are obtained by the combination of holographic lithography and epitaxial growth [1]. Several techniques have been developed to produce nanostructures [2], but the great interest of this one is that small lateral sizes are obtained without the problem of non radiative recombinations on the sidewalls which occur with the classical e-beam lithography/etching method. Heterostructures with GaAs wires have been studied, but it is difficult to integrate these wires in a AlGaAs waveguide because of the presence of aluminium which induces growth defects at the V-groove interface. To avoid this problem, the same technique has been used for InGaAs wires in GaAs waveguides. It is more difficult to provide uniform and high density arrays of wires with low growth defects density as in the first case [3]. Two kinds of structures have been grown: InGaAs quantum wires on [110] V-grooves and InGaAs Distributed FeedBack lasers (DFB) on [1$\bar{1}$0] second order gratings. In this paper, we compare the profil and the behavior of the V-groove in the two crystallographic orientations at different fabrication steps.

2 Fabrication: holographic lithography and MBE growth

The first step consists in the MBE growth of the AlGaAs cladding and the half GaAs waveguide (0.3 μm) on a n-doped (100) GaAs substrate. A grating is obtained on the surface by deep UV holography with a doubled Ar^+ laser at $\lambda = 257$ nm [4]. It comes from the high contrast of the fringes created by the reflection of the laser on a mirror perpendicular to the sample. Its period is determined by the incidence angle of the laser beam. Its reflection on the surface is eliminated by an antireflective coating layer (70 nm thick Si_3N_4). The ratio between the period and the lateral width of the lines depends on the exposure time. In this way, we can influence the etching profile of the

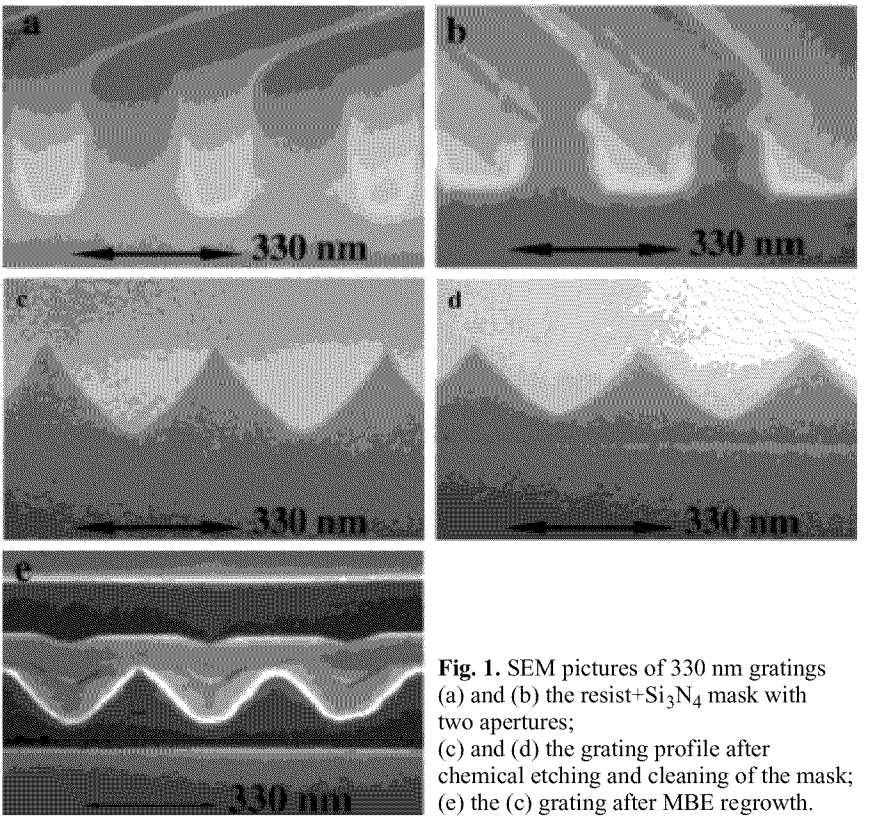

Fig. 1. SEM pictures of 330 nm gratings (a) and (b) the resist+Si_3N_4 mask with two apertures; (c) and (d) the grating profile after chemical etching and cleaning of the mask; (e) the (c) grating after MBE regrowth.

V-grooves, that are described in next section. This mask is transferred from the resist to the Si_3N_4 layer by reactive ion etching with a CF_4/H_2 plasma.

The $[1\bar{1}0]$ V-grooves are etched in commonly used $H_2SO_4/H_2O/H_2O_2$ solution. It develops {111}A facets in this direction, whereas the profile shows an important underetching in the [110] orientation. For this reason the [110] V-grooves are etched in a $CHKO_3/H_2O/H_2O_2$ solution. The grating surface is then protected by a thermic oxide grown at 230°C. Prior to the MBE regrowth, this oxide is removed by a desorption. This interface treatment and the regrown structure depend on the grating orientation.

3 Quantum wires on [110] V-grooves

InGaAs quantum wires have been grown on [110] gratings with periods of 330 nm. The structure consists in a AlAs/GaAs superlattice buffer, a $In_{0.16}Ga_{0.84}As$ quantum wire, an other AlAs/GaAs superlattice, the second part of the GaAs waveguide and the AlGaAs cladding layer. The complete structure has been described elsewhere [5].

SEM micrographs of Fig. 1 show the grating at different fabrication steps, for two ratio between the mask lines and the period: 60% in (a) and 40% in (b). This is obtained by different exposure times. The surfaces formed by the chemical etching are not exactly {111}B facets (As planes), but a combination of planes with higher indices $\{n11\}$ with $n > 1$, which gives this curved profile. The large mask (a) leads to a deeper V-groove (c) than in (d). The grating depths are 190 nm and 130 nm respectively. This

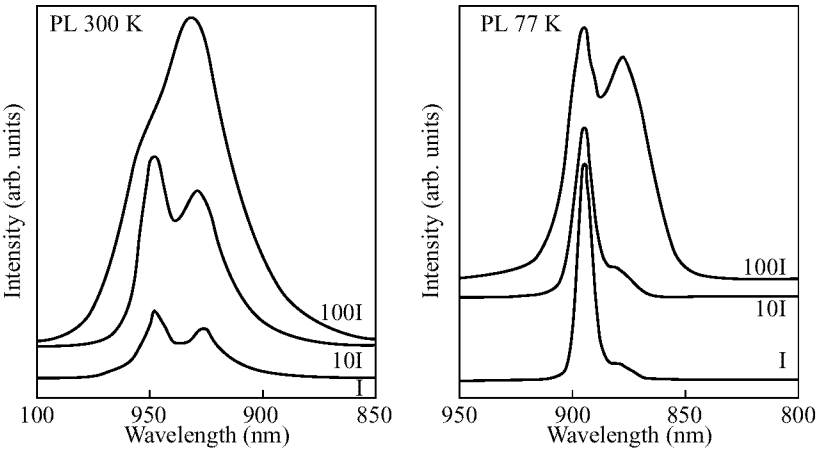

Fig 2. PL spectra of InGaAs wires grown on [110] grating between AlAs/GaAs superlattices at 300 K and 77 K, for three excitation densities.

difference has an influence on the quantum wire shape.

The oxide is removed by thermic desorption at 640°C under As_4 pressure. It reduces processing defects and impurities at the regrowth interface. The result is a rounding of the corners and a lowering of the modulation depth. This phenomenon is more important for shallow etching profiles (d). Differences of adatom diffusion lengths lead to different growth rates on the V-groove facets [6]. The low mobility of Al atoms tends to preserve the shape of the grating, whereas mass transport occurs during the growth interruption following the InGaAs layer that leads to crescent-shape wires [4]. If the same process is done on $[1\bar{1}0]$ gratings, {001} planes are formed on the bottom, and the structure is faster planarized. A SEM picture of the total structure is shown in Fig. 1(e). The layers are revealed by a selective chemical etching of a cleaved surface. The quantum wire is visible by the black line in the middle of the grating structure. On the both sides of the wire, the gray layers represent the AlAs/GaAs superlattices, and black ones the GaAs waveguide. The lower dark layer is the one where the V-grooves are defined. The second GaAs layer, on top of the gray superlattice, is completely planarized. TEM pictures are analyzed in [5]. To understand completely the regrowth characteristics, we have to take into account the evolution of the strain field in these structures.

Photoluminescence spectra of InGaAs wires embedded in AlAs/GaAs superlattices are shown in Fig. 2 for different excitation densities (I, 10I, and 100I). The ground state and the first excited level resulting from the lateral confinement are seen at 948 and 930 nm (PL at 300 K) with a splitting of 17 meV. The spectra exhibit a striking bandfilling with increasing the photogeneration rate as already reported on GaAs wires [7]. The peak associated with the first excited state is very well defined and intense as compared to the ground state, even for low excitation density. This shows the improvement in the control of each fabrication step.

4 Distributed feedback lasers in $[1\bar{1}0]$ V-grooves

Distributed feedback gain-coupled lasers based on InGaAs wires have been grown on [110] gratings [8]. Some efforts have been done on the surface cleaning, but the laser

characteristics are limited by the defects at the regrowth interface. A hydrogen plasma desorption has been developed [9]. It appears that this treatment has a large influence on the grating, but this effect depends on the orientation of the V-grooves. For [110] lines, we observe an important planarization of the surface.

The same process has been used in the $[1\bar{1}0]$ orientation to define second order gratings (280 nm). The chemical etching defines {111}A facets which correspond to Ga planes. In this case, the grating profile is transformed, but the V-grooves are preserved. The difference of the planes, As in [110] and Ga in $[1\bar{1}0]$ explains the behavior specific to the direction. DFB lasers have been grown on $[1\bar{1}0]$ gratings, with a $In_{0.18}Ga_{0.82}As$ quantum well. This active layer is flat, due to the faster planarization in this direction. The structure is defined so that the lateral width of the QW is equal to a 3/4 grating period. Figure 3 shows that the effect of the desorption depends on the etching profile. In (b), the sharpness of the top is more important than in (a). In Fig. 3(c) and 3(d), we see the structure after regrowth on gratings (a) and (b), respectively. The active layer (one or three QWs) is located in the middle of the GaAs waveguide. A AlAs/GaAs superlattice reduces the defects density at the interface. It appears as a gray line following the V-shape. We can compare the evolution of this superlattice for smooth or sharp etching profiles. In the two cases, the {111}A facets are stable, but the top of the grating is different. In (c), the curved top is changed in {311} planes by the desorption. During the regrowth the {111}A planes are reconstructed, as it is shown on TEM micrographs [10], but the {311} based surfaces tend to limit the density of dislocations which may appear at the apex formed by the intersection of the reconstructed {111}A planes. In Fig. 3(d), the sharp grating is not changed by the desorption, and the triangular shape on the top remains constant with the growth. The conservation of the {111}A planes tends to create stacking faults and dislocations emerging from the apex. The efficiency of the desorption depends on the grating shape that is determined by the holographic exposure time and the chemical etching homogeneity. By controlling all theses steps and by using a high quality regrowth we can fabricate reproducible InGaAs DFB laser structures. Threshold current densities as low as 250 A/cm^2 have been achieved at room temperature [9]. We have also grown structures with multiple quantum wells (Fig. 3(d)) to limit the sensitivity to the regrowth interface and to avoid the saturation of the QW luminescence. This should lead to a better reproducibility of the active layer quality and laser properties. A technologic process has been developed to define small stripes of 4 μm on the waveguide cladding, with a $SiCl_4/Cl_2/Ar$ plasma etching followed by a planarization of the surface and the deposition of p-contacts, to increase the current injection in the active layer and reduce the likelyhood of lateral laser modes.

5 Conclusion

The results show the influence of the holographic exposure and chemical etching on the desorption efficiency. We expect a better control of the V-groove profile, and the interface evolution during the desorption and the MBE regrowth, which is important for the reproducibility of the structures and their optical properties. The completely different behavior on the two grating directions [110] and $[1\bar{1}0]$ has been shown. This improvement in the fabrication steps allows to develop the integration in a waveguide of two kinds of InGaAs based structures: quantum wires in [110] V-grooves and DFB

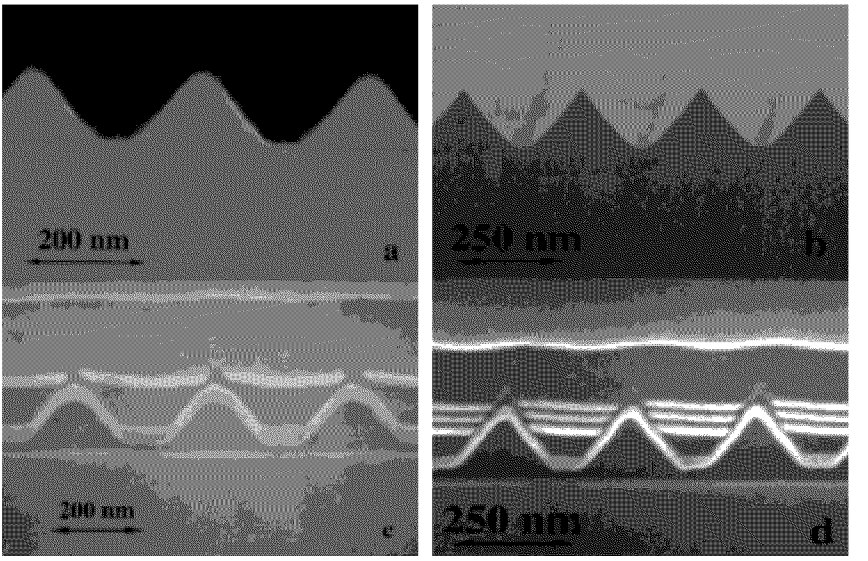

Fig 3. SEM pictures of 280 nm [1$\bar{1}$0] gratings; (a) and (b): Etching profiles. (c) and (d): the same gratings after MBE regrowth.

lasers in [1$\bar{1}$0] gratings. In this second case, structures with three QWs combined with a new process technology should lead to ease the problem of strong threshold current variations.

References

[1] E. Kapon, *Optoelectronics* **8** 429 (1993).
[2] R. Cingolani and R. Rinaldi, *Rivista del Nuovo Cimento*, 16, 1993.
[3] P. H. Jouneau, F. Bobard, U. Marti, J. Robadey, F. Filipowitz, D. Martin, F. Morier-Genoud, P. C. Silva, Y. Magnenat and F. K. Reinhart, *Inst. Phys. Conf. Ser.* **146** 371 (1995).
[4] U. Marti, M. Proctor, D. Martin, F. Morier-Genoud, B. Senior and F. K. Reinhart, *Microelectronics Eng.* **13** 391 (1991).
[5] F. Filipowitz, present conference.
[6] F. S. Turco, S. Simhony, K. Kash, D. M. Hwang, T. S. Ravi, E. Kapon and M. C. Tamargo, *J. Cryst. Growth* **104** 766 (1990).
[7] R. Rinaldi, M. Ferrara, R. Cingolani, U. Marti, D. Martin, F. Morier-Genoud, P. Ruterana and F. K. Reinhart, *Phys. Rev. B* **50** 11795 (1994).
[8] J. Robadey, U. Marti, R. O. Miles, M. Glick, F. Filipowitz, M. Achtenhagen, D. Martin, F. Morier-Genoud, P. C. Silva, Y. Magnenat, P. H. Jouneau, F. Bobard and F. K. Reinhart, *IEEE Photonics Technol. Lett.* **9** (1) 5 (1997).
[9] J. Robadey, D. Martin, M. Glick, P. C. Silva, P. H. Jouneau, U. Marti and F. K. Reinhart *Electronics Lett.* **33** (4) 297 (1997).
[10] J. Robadey et al. (to be published).